

Anisotropy of the Hubble Constant in a Cosmological Model with a Local Void on Scales of ~ 200 Mpc

Kenji TOMITA

Yukawa Institute for Theoretical Physics, Kyoto University, Kyoto 606-8502

A spherical cosmological model with a local void on scales of ~ 200 Mpc and with an inhomogeneous Hubble constant was proposed in recent two papers. This model explains consistently the observed properties of the cosmic bulk flow, the accelerating behavior of type Ia supernovae and the CMB dipole anisotropy without invoking a cosmological constant. As we are in a position deviated from the center in the model, the anisotropy of the Hubble constant appears owing to the directional difference of the distance from the observer to the boundary of the void region. It is found that the anisotropy is maximally about 6 % of the constant in the region of $200 \sim 500$ Mpc from us. This inhomogeneity and anisotropy of the Hubble constant are not so large as to be inconsistent with the present observation. The detection of this anisotropy in the future will be useful to clarify the implication of the inhomogeneity of the Hubble constant.

§1. Introduction

A spherical cosmological model with a local void on scales of ~ 200 Mpc was proposed in our recent papers,¹⁾⁻²⁾ (cited as Paper 1 and Paper 2, respectively), to explain consistently the observed properties of the cosmic bulk flow, the accelerating behavior of type Ia supernovae (SNIa) and the CMB dipole anisotropy, without invoking a cosmological constant. In this model the Hubble constant is inhomogeneous. Here we will derive the anisotropy of the constant associated with the inhomogeneity and discuss its consistency with the present observed values of the Hubble constant.

The deviation of local expansion rates H_L from the global Hubble constant H_0 due to small-scale perturbations and large-scale structures of the universe has so far been studied by many people from various viewpoints. Here, let us briefly review the long history of these studies. First, Turner et al.³⁾ derived the probability distribution function of H_0 with given H_L using numerical simulations, and Suto et al.⁴⁾ and Nakamura and Suto⁵⁾ obtained it analytically in a simple model of inhomogeneities with a local low-density region. It was found as a result that the probability of a large deviation such as $(H_L - H_0)/H_L > 0.4$ is very small for inhomogeneities with the radii $\sim 100h^{-1}$ Mpc, where $H_0 = 100h$ km s⁻¹ Mpc⁻¹. In the linear analyses using power spectra in the CDM models, moreover, Shi and Turner⁷⁾ and Wang et al.⁸⁾ showed that the cosmic and sample variances of $(H_L - H_0)/H_0$ are $\sim 0.4\%$ for the samples extending to $\sim 100h^{-1}$ Mpc.

Second, the behavior of CMB dipole anisotropy was discussed to derive the constraints upon structures with inhomogeneous expansion rates by Nakao et al.⁹⁾, Tomita^{10)-11) 1)}, Shi et al.⁶⁾, Shi and Turner⁷⁾, Humphreys et al.¹²⁾, and Wang et al.⁸⁾, where the anisotropy was assumed to be measured by an off-center observer in spherical models with an inner low-density region enclosed by an outer homoge-

neous region. When we consider only the redshift arising from the observer's peculiar motion relative to the CMB rest frame, the dipole component is found to be unacceptably large for the radius of the low-density region $\sim 200h^{-1}$ Mpc. The present author, however, showed^{1) 11)} by solving exactly the null-geodesic equations from the off-center observer to the last-scattering surface, that in the spherical models, not only the redshift from the observer's relative motion, but also the gravitational redshift are effective, and their main terms are cancelled out, so that the total dipole component is small compared with the component only from the relative motion, and reduces to about 1/10 of the latter component, as long as he is near the center. Because of this special situation, spherical structures on the scale $\sim 200h^{-1}$ with $H_0/H_L \sim 0.8$ are not constrained by the observed value of CMB dipole anisotropy.

Third, the models with inhomogeneous expansion rates have been studied in connection with the spatial distribution and the $[m, z]$ relation of type I supernovae (SNIa) by Wu et al.,¹³⁾ Wu et al.,¹⁴⁾ Zehavi et al.¹⁵⁾ and Tomita.²⁾ Zehavi et al.¹⁵⁾ investigated the local inhomogeneity on the scale of $\sim 60h^{-1}$ Mpc around the Local Group as a model of the *Hubble bubble*. However, it contradicts with the observational result of Giovanelli et al.¹⁶⁾ which shows that the Hubble flow is uniform in the region within $100h^{-1}$ Mpc.

Independently of their model, the present author proposed another spherical model (the *cosmological void model*), which consists of the inner homogeneous region (on the scale of $\sim 200h^{-1}$ Mpc) and the outer homogeneous region with different Hubble constants (Paper 1 and Paper 2). It was introduced to explain the puzzling situation in the cosmic bulk flow on the scale of $\sim 150h^{-1}$ Mpc that was observed by Hudson et al.¹⁷⁾ and Willick.¹⁸⁾ Their observational results are not compatible with the other observations (Dale et al.,¹⁹⁾ Giovanelli et al.,²⁰⁾ and Riess et al.²¹⁾ in homogeneous cosmological models, as was discussed by many people in the Workshop of Cosmic Flows (S. Courteau et al. 1999), but they may be compatible with them in our inhomogeneous model (Tomita²²⁾). This is because (a) in the inner homogeneous region there is no peculiar motion between comoving observers and clusters, (b) the off-center observers find a systematic motion of comoving clusters in the inner region relative to the global expansion, and (c) the total CMB dipole anisotropy measured by the off-center observers is small, and so the off-center observers in the inner region feel as if they were in the CMB rest frame, in spite of their motions relative to the global expansion. Thus our inhomogeneous model may explain the puzzling situation in the bulk flow, though the probability of its realization is very small.

It was also shown that this model can explain the accelerating behavior of high-redshift supernovae, without a cosmological constant. It does not contradict with Giovanelli et al.'s result, because the diameter of the inner region is much larger than the size of their observed region $100h^{-1}$ Mpc.

The local values of the Hubble constant have recently been measured by the HST Key Project (Sakai et al.²³⁾), the High-z Supernova Search Team,²⁴⁾ and Tutui et al.²⁵⁾ using the common calibrations due to Cepheid stars. The measurement in the first group using the multi-wavelength Tully-Fisher relation is limited to the region within $100h^{-1}$ Mpc and the obtained median value is $71 \text{ km s}^{-1} \text{ Mpc}^{-1}$. The unit $\text{km s}^{-1} \text{ Mpc}^{-1}$ is omitted in the following for simplicity. The measurements in the

second group were done in the region reaching $400h^{-1}$ Mpc, and the median value is 64. Those in the third group were performed using the CO Tully-Fisher relation (Sofue et al.^{26) 27)} in the region between 100 and $400h^{-1}$ Mpc and the median value is 61. All of these values have errors of the order of ± 10 , but it seems that these locally measured values of the Hubble constant have the tendency to decrease with the increase of the distance.

In view of the above studies we derive in this paper the effective Hubble constant (corresponding to the observed constant) in the above inhomogeneous models with a local void and study the anisotropy which will be observed by an off-center observer. The detection of this anisotropy will be useful to consider the implication of observed inhomogeneity of the Hubble constant.

§2. Effective Hubble constant

Various spherical inhomogeneous models (i.e. single-shell models, multi-shell models and models with a self-similar region) were considered in Paper 1. Here we treat only the simplest model consisting of the inner low-density homogeneous region (V^I) and the outer high-density homogeneous region (V^{II}) connected with a single shell. The density parameters and Hubble constants in V^I and V^{II} are denoted as (Ω_0^I, H_0^I) and $(\Omega_0^{II}, H_0^{II})$, respectively, where $H_0^l = 100h^l$ ($l = I$ or II). Here we assume $\Omega_0^I < \Omega_0^{II}$ and $H_0^I > H_0^{II}$. The typical Hubble constant is $H_0^I = 71$ and $H_0^{II} = 57$ ($= 0.8 \times H_0^I$). The radius of the shell and the distance from the center C to our observer are assumed to be $200(h^I)^{-1}$ Mpc and $40(h^I)^{-1}$ Mpc, as in previous papers.

In this paper we consider the local behavior of light rays (reaching the observer) in the near region within 500 Mpc around O, and so the distance is expressed using the lowest-order terms of the expansion with respect to z (≤ 0.15). In contrast with the description in previous papers, the paths are expressed using polar coordinates (r, ϕ, θ) with the origin O, as in Fig.1.

The center C has the coordinates $r = r_c$ and $\phi = \pi$. In these coordinates the line-element in V^I and V^{II} are expressed as

$$ds^2 = -c^2(dt^l)^2 + [a^l(t^l)]^2 \left\{ (dr^l)^2 + [\sinh r^l]^2 d\Omega^2 \right\}, \quad (2.1)$$

where $l = I$ or II and $d\Omega^2 = d\phi^2 + \sin^2 \phi d\theta^2$. The shell is given by $r^l = r_b^l(\phi)$, which depends on time t^l , but its time dependence is neglected in the calculation of light paths, because $(a^l dr_b^l / dt^l) / c$ ($\sim 10^{-2}$) is very small and the time difference for rays with $\phi = 0$ and π is also very small.

In V^I all rays reaching O are radial and straight, because of homogeneity in V^I , and we have the relation

$$\frac{1}{1+z^I} = \frac{a^I(t^I)}{a^I(t_0^I)} = 1 + \left(\frac{\dot{a}^I}{a^I} \right)_0 (t^I - t_0^I) \quad (2.2)$$

or

$$c(t_0^I - t^I) = z^I c / H_0^I \quad (2.3)$$

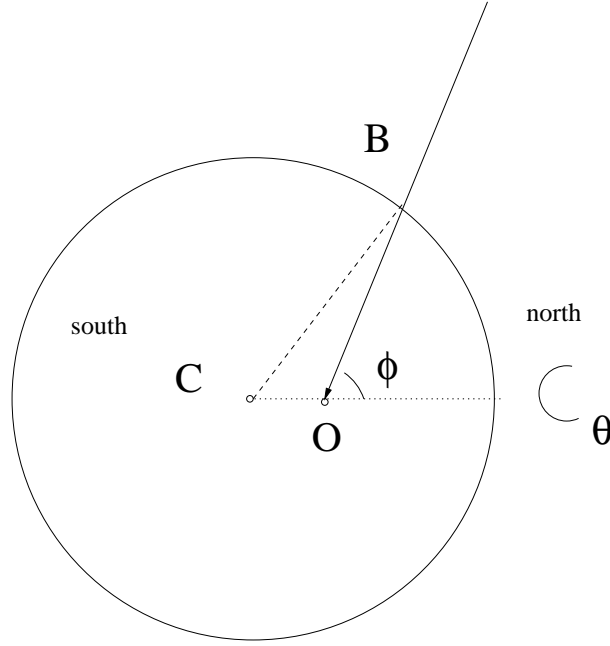


Fig. 1. A model with a single shell.

between the origin and the boundary, where $H_0^I \equiv (\dot{a}^I/a^I)_0$. In the above equations we neglected the terms of $O(t^I - t_0^I)^2$. Then we have at the boundary

$$c(t_0^I - t_1^I) = z_1^I c/H_0^I. \quad (2.4)$$

The direction of light rays changes at the boundary in general, but the amplitude of their change is small and of the order of $\sinh r - r \approx r^3 \approx (z^{\text{II}})^3$, which is neglected in the present approximation. Accordingly the light rays are regarded as straight, also in V^{II} , and so in V^{II} we have the relation

$$\frac{1 + z^{\text{II}}}{1 + z_1^{\text{II}}} = \frac{a^{\text{II}}(t_1^{\text{II}})}{a^{\text{II}}(t^{\text{II}})} = 1 + \left(\frac{\dot{a}^{\text{II}}}{a^{\text{II}}}\right)_1 (t_1^{\text{II}} - t^{\text{II}}) \quad (2.5)$$

or

$$c(t_1^{\text{II}} - t^{\text{II}}) = (z^{\text{II}} - z_1^{\text{II}}) c/H_1^{\text{II}}, \quad (2.6)$$

where we neglected similarly the terms of $O(t^{\text{II}} - t_1^{\text{II}})^2$. Because $H_1^{\text{II}} - H_0^{\text{II}} \approx O(z_1^{\text{I}})$, we can use H_0^{II} in place of H_1^{II} in the present approximation, and so we obtain

$$c(t_1^{\text{II}} - t^{\text{II}}) = (z^{\text{II}} - z_1^{\text{II}}) c/H_0^{\text{II}}. \quad (2.7)$$

At the boundary the equality $z_1^{\text{I}} = z_1^{\text{II}}$ holds due to the junction condition that the lapses of times t^{I} and t^{II} are continuous (cf. Paper I). In the following we put $z_1^{\text{I}} (= z_1^{\text{II}})$, z^{I} , z^{II} as z_1 , z , z for simplicity. The ϕ dependence of the boundary is shown later.

Accordingly the distance D between the observer and the source with redshift z is

$$D (= c(t_0^{\text{I}} - t^{\text{I}})) = z c/H_0^{\text{I}} \quad \text{for } z \leq z_1(\phi) \quad (2.8)$$

and

$$D(= c(t_0^I - t_1^I) + c(t_1^{II} - t^{II})) = z_1 c/H_0^I + (z - z_1) c/H_0^{II} \quad \text{for } z > z_1(\phi). \quad (2.9)$$

At the boundary we have

$$D_1(\phi) = z_1(\phi) c/H_0^I. \quad (2.10)$$

Here we define the effective Hubble constant H_0^{eff} , which corresponds to the observed Hubble constant, by

$$D = z c/H_0^{\text{eff}}. \quad (2.11)$$

Then $H_0^{\text{eff}} = H_0^I$ for $z < z_1$, and

$$\frac{H_0^I}{H_0^{\text{eff}}} = \frac{H_0^I}{H_0^{II}} - \left(\frac{H_0^I}{H_0^{II}} - 1 \right) \frac{z_1}{z} \quad (2.12)$$

for $z \geq z_1$. If we eliminate z using Eqs. (2.9) and (2.10), we obtain

$$H_0^{\text{eff}} = H_0^{II} + (H_0^I - H_0^{II})D_1(\phi)/D \quad (2.13)$$

for $z \geq z_1$.

Next the functional form of $D_1(\phi)$ is given. In terms of the distance D_b (between C and a point B on the boundary) and the distance D_o (between C and O), we obtain

$$D_1(\phi) = \left[D_b^2 - D_o^2 \sin^2 \phi \right]^{1/2} - D_o \cos \phi \quad (2.14)$$

from the geometrical analysis in ΔCOB in Fig.1. If $D < D_b - D_o$ or $D > D_b + D_o$, we have $D < \text{or } > D_1(\phi)$ for all ϕ . If $D_b + D_o > D > D_b - D_o$, we have $D = D_1(\phi)$ for $\phi = \phi_1$ specified by

$$\mu_1 \equiv \cos \phi_1 \equiv \frac{D_c^2 - D^2}{2D_o D}, \quad (2.15)$$

where $D_c \equiv (D_b^2 - D_o^2)^{1/2}$.

The expressions of the effective Hubble constant are given as follows (cf. Fig.2).

(1) For $D \leq D_b - D_o$,

$$H_0^{\text{eff}} = H_0^I. \quad (2.16)$$

(2) For $D_b + D_o > D > D_b - D_o$,

$$H_0^{\text{eff}} = H_0^I \quad \text{for } \phi \geq \phi_1 \quad (2.17)$$

and otherwise H_0^{eff} is given by Eq. (2.13).

(3) For $D \geq D_b + D_o$, H_0^{eff} is given by Eq. (2.13) similarly.

In the case of (2) and (3), H_0^{eff} has the minimum and maximum at $\phi = 0$ and π , respectively.

Now let us consider the angular average of the effective Hubble constant ($\langle H_0^{\text{eff}} \rangle$) for (2) and (3). It is defined by

$$\langle H_0^{\text{eff}} \rangle = H_0^{II} + \frac{H_0^I - H_0^{II}}{D} I, \quad (2.18)$$

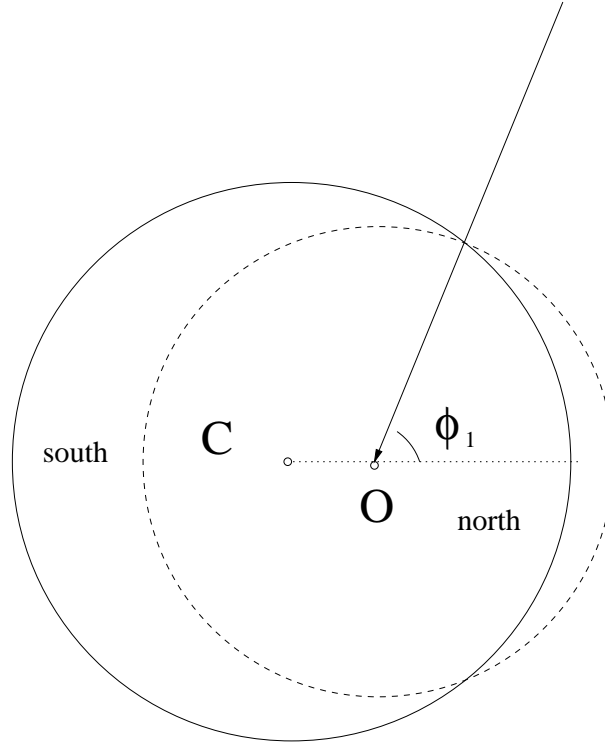


Fig. 2. A surface with $D = \text{const.}$ in the case of $D_c + D_o > D > D_c - D_o$.

where

$$I \equiv \int_{\phi_a}^{\phi_b} \text{Min}[D, D_1(\phi)] d \cos \phi / \int_{\phi_a}^{\phi_b} d \cos \phi \quad (2 \cdot 19)$$

for the average interval $[\phi_a, \phi_b]$. As examples we consider the whole-sky average ($\phi_a = 0, \phi_b = \pi$), the northern-sky average ($\phi_a = 0, \phi_b = \pi/2$), and the southern-sky average ($\phi_a = \pi/2, \phi_b = \pi$). Here the north is taken to be in the direction of $C \rightarrow O$. The integrals (I) corresponding to their averages are denoted as $I_A(i)$, $I_N(i)$ and $I_S(i)$, respectively, in which $i = 2$ and 3 for the above cases (2) and (3), respectively. The expressions of these integrals are given in Appendix A.

The maximum and minimum values of H_0^{eff} (for $\phi = \pi$ and $\phi = 0$) and the values $\langle H_0^{\text{eff}} \rangle_i$ for whole-, northern- and southern-sky averages ($i = A, N$ and S) were calculated in a typical example of $D_o = 40(h^I)^{-1}$ Mpc, $D_b = 5D_o$, $H_0^I = 71$ and $H_0^{II} = 57$, which were assumed in our previous papers. Their behaviors are shown in Fig. 3.

As a result it is found that

- (1) The whole-sky average $\langle H_0^{\text{eff}} \rangle_A$ is constant in $D < D_b - D_o$, and decreases gradually from 71 (for $D = D_b - D_o$) to 62 (for $D \sim 500(h^I)^{-1}$ Mpc),
- (2) The difference between $\langle H_0^{\text{eff}} \rangle_N$ and $\langle H_0^{\text{eff}} \rangle_S$ is about $(2.5 \sim 1.3)$ for $D = (160 \sim 500)(h^I)^{-1}$ Mpc,
- (3) The difference between the maximum and minimum values of H_0^{eff} is about $(4.0 \sim 2.5)$ for $D = (160 \sim 500)(h^I)^{-1}$ Mpc.

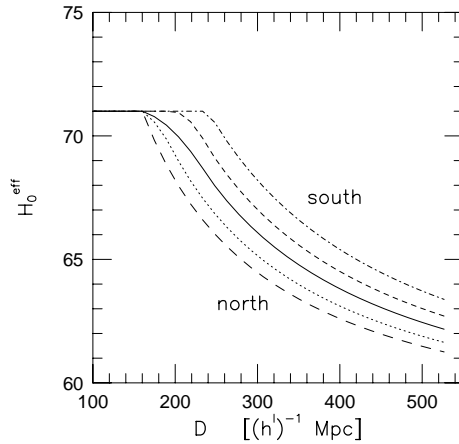


Fig. 3. A diagram of the effective Hubble constant H_0^{eff} ($\text{km s}^{-1} \text{Mpc}^{-1}$) and the distance D (Mpc). The lines show the maximum, the southern-sky average, the whole-sky average, the northern-sky average, and the minimum in the order from top to bottom.

These behaviors of H_0^{eff} seem to be consistent with the dispersive but decreasing tendency of the observed Hubble constant.

§3. Concluding remarks

If there is a spherical inhomogeneity in the Hubble constant, the anisotropy in it and the bulk flow relative to the global expansion necessarily occur, as long as our observer is not in the center. If this bulk flow is the one found by Hudson et al. and Willick, the corresponding anisotropy should be detected in the same direction, by the observations of nearby SNIa and galaxies (through CO Tully-Fisher method). Then the north is in the direction of the cosmic bulk flow, that is, $l = 260 \pm 15^\circ$, $b = -1 \pm 12^\circ$ (Hudson et al. 1999), or $l = 266^\circ$, $b = 19^\circ$ with 1σ error (Willick 1999).

In this paper we assumed the simplest *cosmological void models*, in which the Hubble constant changes abruptly at the boundary. If we assume smoother models with a self-similar intermediate region, the change in the effective Hubble constant also may be somewhat slower.

With the present assumption, considering only the lowest-order terms with respect to z , the dependence on the density parameter was neglected. The nonlinear full treatment with respect to z was given in Paper 2 and the [distance - z] relation was found to be consistent with SNIa data.

Here a few comments are added as for our void. It refers to the low-density region (V^I) with respect to the total matter density. The galactic number densities in the two regions V^I and V^{II} depend on the different complicated histories of galaxy formation, and their difference at the boundary may be rather small compared to the difference of total densities.

Appendix A

— Integrals for the averaging —

The integrals (I) for the whole-sky average ($\phi_a = 0, \phi_b = \pi$) for the cases (2) and (3) are

$$I_A(2) = \frac{1}{4} \left[2D(\mu_1 + 1) + D_o(J_1 - J_2) \right], \quad (\text{A}\cdot 1)$$

where

$$J_1 \equiv \left[\left(\frac{D_c}{D_o} \right)^2 - 1 \right]^{1/2} + \left(\frac{D_c}{D_o} \right)^2 \sin^{-1} \frac{D_o}{D_c} - 1, \quad (\text{A}\cdot 2)$$

$$J_2 \equiv \mu_1 \left[\left(\frac{D_c}{D_o} \right)^2 - (\mu_1)^2 \right]^{1/2} + \left(\frac{D_c}{D_o} \right)^2 \sin^{-1} \frac{\mu_1 D_o}{D_c} - (\mu_1)^2, \quad (\text{A}\cdot 3)$$

and

$$I_A(3) = \frac{1}{2} D_o \left\{ \left[\left(\frac{D_c}{D_o} \right)^2 - 1 \right]^{1/2} + \left(\frac{D_c}{D_o} \right)^2 \sin^{-1} \frac{D_o}{D_c} \right\}. \quad (\text{A}\cdot 4)$$

The integrals I for the northern-sky average ($\phi_a = 0, \phi_b = \pi/2$) and the southern-sky average ($\phi_a = \pi/2, \phi_b = \pi$) are expressed as $I_N(i)$ and $I_S(i)$, respectively, with $i = 2$ and 3. Here the north is taken to be in the direction of $C \rightarrow O$.

For $D_c > D > D_b - D_o$,

$$I_N(2) = \frac{1}{2} D_o \left[J_1 - J_2 \right] + D\mu_1, \quad (\text{A}\cdot 5)$$

$$I_S(2) = D. \quad (\text{A}\cdot 6)$$

For $D_b - D_o > D > D_c$,

$$I_N(2) = \frac{1}{2} D_o J_1, \quad (\text{A}\cdot 7)$$

$$I_S(2) = D(\mu_1 + 1) - \frac{1}{2}D_o J_2. \quad (\text{A}\cdot 8)$$

For $D > D_b + D_o$,

$$I_N(3) = I_A(3) - \frac{1}{2}D_o, \quad (\text{A}\cdot 9)$$

$$I_S(3) = I_A(3) + \frac{1}{2}D_o. \quad (\text{A}\cdot 10)$$

The author is grateful to Prof. T.P. Singh for his careful reading of the manuscript. This work was supported by Grant-in Aid for Scientific Research (No. 10640266) from the Ministry of Education, Science, Sports and Culture, Japan.

References

- [1] K. Tomita, *Astrophys. J.* **529** (2000), 26, cited as Paper 1
- [2] K. Tomita, *Astrophys. J.* **529** (2000), 38, cited as Paper 2
- [3] E.I. Turner, R. Cen, and J.P. Ostriker, *Astron. J.* **103** (1992), 1427
- [4] Y. Suto, T. Sugihara, and Y. Inagaki, *Prog. Theor. Phys.* **93** (1995), 839
- [5] T.T. Nakamura and Y. Suto, *Astrophys. J.* **447** (1995), L65
- [6] X. Shi, L.M. Widrow, and L.J. Dursi, *Month. Notices R.A.S.* **281** (1996), 565
- [7] X. Shi and M.S. Turner, *Astrophys. J.* **493** (1998), 519
- [8] Y. Wang, D.N. Spergel, and E.L. Turner, *Astrophys. J.* **498** (1998), 1
- [9] K. Nakao, N. Gouda, T. Chiba, S. Ikeuchi, T. Nakamura, and M. Shibata, *Astrophys. J.* **453** (1995), 541
- [10] K. Tomita, *Astrophys. J.* **451** (1995), 1
- [11] K. Tomita, *Astrophys. J.* **461** (1996), 507
- [12] N.P. Humphreys, R. Maartens, R., and D.R. Matravers, *Astrophys. J.* **477** (1997), 47
- [13] X.-P. Wu, Z. Deng, Z. Zou, L.-Z. Fang, and B. Qin, *Astrophys. J.* **448** (1995), L65
- [14] X.-P. Wu, B. Qin, L.-Z. Fang, *Astrophys. J.* **469** (1996), 48
- [15] I. Zehavi, A. G. Riess, P. Kirshner, and A. Dekel, *Astrophys. J.* **503** (1998), 483
- [16] R. Giovanelli, D.A. Dale, M.P. Haynes, E. Hardy, and L.E. Campusano, *Astrophys. J.* **525** (1999), 25
- [17] M. J. Hudson, R. J. Smith, R.J., J. R. Lucey, D. J. Schlegel and R. L. Davies, *Astrophys. J.* **512** (1999), L79
- [18] J. A. Willick, *Astrophys. J.* **522** (1999), 647
- [19] D. A. Dale, R. Giovanelli, and M.P. Haynes, *Astrophys. J.* **510** (1999), L11
- [20] R. Giovanelli, M. P. Haynes, W. Freudling, L. N. da Costa, J. J. Salzer, and G. Wegner, *Astrophys. J.* **505** (1998), L91
- [21] A. G. Riess, M. Davis, J. Baker, and R. P. Kirshner, *Astrophys. J.* **488** (1997), L1
- [22] K. Tomita, K. in *Proc. Cosmic Flows Workshop*, eds. S. Courteau, M. Strauss, and J. Willick (ASP, Canada, 1999), 302
- [23] S. Sakai et al., *Astrophys. J.* **529** (2000), 698
- [24] S. Jha et al. *Astrophys. J. Suppl.* **125** (1999), 73
- [25] Y. Tutui et al., *Publ. Astron. Soc. Japan* (2000) in preparation
- [26] Y. Sufue et al., *Publ. Astron. Soc. Japan* **48** (1996), 657
- [27] Y. Tutui and Y. Sufue, *Astron. Astrophys.* **351** (1999), 467